CrossMark

ORIGINAL PAPER

Photocrosslinked methacrylated chitosan-based nanofibrous scaffolds as potential skin substitute

Yingshan Zhou · Kaili Liang · Can Zhang · Jun Li · Hongjun Yang · Xin Liu · Xianze Yin · Dongzhi Chen · Weilin Xu · Pu Xiao

Abstract Nanofibers based on natural polymers have recently been attracting research interest as promising materials for use as skin substitutes. Here, we prepared photocrosslinked nanofibrous scaffolds based on methacrylated chitosan (MACS) by photocrosslinking electrospun methacrylated chitosan/ poly (vinyl alcohol) (PVA) mats and subsequently removing PVA from the nanofibers. We comprehensively investigated the solution properties of MACS/ PVA precursors, the intermolecular action between MACS and PVA components, and the morphology of MACS/PVA nanofibers. Results indicated that the fiber diameter and morphology of the photocrosslinked methacrylated chitosan-based nanofibrous scaffolds were controlled by the MACS/PVA mass ratio and showed highly micro-porous structures with many fibrils. In vitro cytotoxicity evaluation and cell culture experiments confirmed that MACS-based mats with micro-pore structure were biocompatible with L929 cells and facilitated cellular migration into the 3D matrix, demonstrating their potential application as skin replacements for wound repair.

Y. Zhou (✉) · K. Liang · C. Zhang ·
J. Li · H. Yang · X. Liu · X. Yin · D. Chen · W. Xu
College of Materials Science and Engineering, Wuhan Textile University, Wuhan 430073, People's Republic of China
e-mail: zyssyz@126.com

P. Xiao (✉)
Centre for Advanced Macromolecular Design, School of Chemistry, University of New South Wales, Sydney, NSW 2052, Australia
e-mail: p.xiao@unsw.edu.au

Introduction

Traumatic wounds are often caused by fire, chemicals or diseases (Zhou et al. 2008). Clinically, skin substitutes are used as covers to prevent excessive fluid loss from open wounds while allowing oxygen transport, as well as creating a moist environment for promoting wound epithelialization. Such skin substitutes must also meet the requirement of biocompatibility. Nanofibers based on natural polymers have been attracting a great deal of interest as promising skin scaffolds thanks to their high porosity, large surface to volume ratio (Ding et al. 2014; Rieger et al. 2013) and low immunogenicity (Lee et al. 2009), . Electrospinning, a simple and multifarious technique, is commonly applied to fabricate nanofibers as potential skin substitutes from natural polymers including chitosan (Antunes et al. 2015), alginate (Leung et al. 2014), silk fibroin (Song et al. 2016), gelatin (Li et al.

2016a, b) and hyaluronic acid (Uppal et al. 2011). Chitosan (CS), is a derivative of chitin, which is the second most abundant polysaccharide in nature, next to cellulose (Tang et al. 2016). It is regarded as one such polymer that fulfils the requirement for a skin substitute, owing to its antimicrobial character, biocompatibility and biodegradability (Li et al. 2016a, b). In this capacity, chitosan can help wounds heal faster and prevent scarring (Anjum et al. 2016).

In the last few years, chitosan-based nanofibers have been successfully prepared by electrospinning of homogeneous chitosan (Ohkawa et al. 2004) or chitosan solutions blended with poly (ethylene oxide) (PEO) (Bhattarai et al. 2005), poly (vinyl alcohol) (PVA) (Zhou et al. 2006), or silk fibroin (Zhang et al. 2011). However, some toxic solvents such as trifluoroacetic acid, acrylic acid, 1,1,1,3,3,3-hexafluoro-2-propanol, and dimethyl sulfoxide have usually been involved in the preparation of these chitosan-based nanofibers, which limited their applications for wounded skin. To reduce the toxicity while enhancing the biocompatibility, much effort has been devoted to electrospinning water-soluble chitosan derivatives (Alipour et al. 2009; Zarandi et al. 2015; Zhou et al. 2008) into nanofibers. However, there is a major drawback with these water-soluble fibrous mats: rapid hydrolysis makes it difficult to for the mat to remain intact in the physiological environment, rendering water-soluble mats unfit for use as tissue engineering scaffolds. To prevent rapid hydrolysis, it is necessary to chemically crosslink these water-soluble fibers. Additionally, although electrospun nanofibers have fibrous porous structures which can mimic the size scale of the native extracellular matrix, one limitation for the nanofiber scaffolds is a relatively small pore size, and the resultant difficulty for cell infiltration, which retards tissue remodeling (Kurpinski et al. 2010; Sundararaghavan et al. 2010).

To address these issues, we prepared photocrosslinkable methacrylated chitosan-based nanofibrous scaffolds with micrometer size pores by PVA-aiding electrospinning, then subsequently extracted PVA from the nanofibers. Here, water was used as the solvent for MACS, which is ideal for medical applications thanks to the absence of toxic residues. Photocrosslinked MACS-based mats have micrometer size pores that can favor cell infiltration to form three-dimensional skin tissues. In addition, their nanofibrillar structures resemble the natural extracellular matrix, which favors the attachment of cells (Bhattarai et al. 2005). Finally, high specific surface area and porosity can guarantee gaseous exchange and removal of excess exudates, which also encourages wound healing (Jayakumar et al. 2011). We also characterized morphology and thermal properties. The in vitro cytotoxicity of photocrosslinked MACS-based mats iswas evaluated with L929 cells. Cellular infiltration was evaluated with DNA plasmid encoding green fluorescent protein transfected Human Embryonic Kidney 293T (HEK 293T) cells used as model cells.

Experimental

Materials

Chitosan (Mw = 1.0×10^5 Da) was purchased from Zhejiang Golden-Shell Biochemical Co., Ltd., China. The deacetylation degree of chitosan was determined to be 67.2% by ^{1}H NMR (Hirai et al. 1991). Poly (vinyl alcohol) (1.7×10^5 Da, 88% hydrolyzed) was obtained from Kuraray Co, Ltd., Japan. 2-Hydroxyethyl methacrylate (HEMA) was obtained from Tianjin Institute of Chemical Reagents. Acryloyl chloride was obtained from Shanghai Chemical Reagents Company, China. Darocur 2959 (D-2959, 2-hydroxy-1-[4-(hydroxyethoxy) phenyl]-2-methyl-1-propanone) was donated from IGM Resins B.V. (Netherlands). Mouse fibroblasts (L929) were purchased from Wuhan Beinglay Biological Technology Co., Ltd., China. DNA plasmid encoding green fluorescent protein transfected Human Embryonic Kidney 293T (HEK 293T) cells were kindly provided by the Institute of Hydrobiology, Chinese Academy of Sciences.

Synthesis of methacrylated chitosan (MACS)

Water-soluble methacrylated chitosan was prepared as described in our previous report (Gao et al. 2010). Briefly, 83.81 g HEMA, 105 mL triethylamine and 9.79 g acryloyl chloride were mixed in 300 mL toluene and reacted under a temperature of 0–5 °C for 12 h. Then, the mixture was filtered and extracted with water, 1 mol L^{-1} HCl and 1 mol L^{-1} NaHCO$_3$ solution, respectively. After that, ethylene glycol acrylate methacrylate (EGAMA, yellow liquid) was obtained by removing the toluene.

Then, 2.0 g chitosan, 0.69 mL acetic acid and 4.0 g EGAMA were mixed in water/ethanol (5:4) solution (90 mL) and reacted for 2 days at 60 °C. After that, $NaHCO_3$ was added to the mixture solution, which then was dialyzed against water and lyophilized to get pure MACS. ^{1}H NMR spectroscopy was recorded in CD_3COOD/D_2O as solvents on a Bruker AV 400 NMR instrument.

Preparation of MACS/PVA solutions

We prepared 15% (w/v) MACS solution and 10% (w/v) PVA solution. The MACS solution was combined with the PVA solution at MACS/PVA mass ratios of 100/0, 75/25, 50/50, 25/75, and 0/100.

The conductivity of the MACS/PVA solution was evaluated by electrical conductivity meter (DDB-6200, Shanghai Rex Xinjing Instrument Co. Ltd., China), and the viscosity of the MACS/PVA solution was examined as shear rate of $\sim 400 \ s^{-1}$ on an AR 2000ex rheometer (TA Instrument, USA) by using a steel parallel plate geometry with a diameter of 40 mm and a 1 mm gap at 25 °C.

Preparation of electrospun membranes

The electrospinning set-up was composed of a 20 mL plastic syringe with a stainless needle (0.57 mm inner diameter), grounded aluminum foil as the collector and a high voltage–power supply (EST705, Beijing Huajinghui Technology Co., Ltd., China). A voltage of 25 kV dc and 12 cm distance was applied between the needle and the plate; the solution flow rate was 1.0 mL/h.

Photocrosslinking of the nanofibers

For further photopolymerization, the MACS/PVA solution at MACS/PVA mass ratio of 50/50 was prepared containing cytocompatible UV photoinitiator D-2959 (0.1 w/v %) (Williams et al. 2005). The nanofiber mats were obtained by the aforementioned electrospinning process and irradiated directly under a 250 W Hg lamp with a light intensity of 30 mW/cm^{2} for 30 min. Upon UV irradiation, the photoinitiator in the mats initiated further crosslinking of MACS nanofiber mats. The photocrosslinked nanofibrous mats were collected and then dried at 25 °C in z vacuum for 12 h. After the photocrosslinking process,

the electrospun nanofibrous scaffold was soaked in purified water for 48 h at 37 °C, refreshing water daily to remove PVA. The mats were lyophilized and the morphology was observed by SEM. These lyophilized mats (photocrosslinked MACS-based nanofibers) were used for subsequent MTT evaluation and cell culture study.

Characterizations

Morphology of the nanofibers

A scanning electron microscope (JSM-6510, JEOL Ltd., Japan) was used to evaluate the basic characteristics of the nanofibers, such as fiber morphology and diameter. The accelerated voltage was 10 kV. The diameters of nanofibers in SEM Images were measured using an image analyzer (Image J, version 1.37 v, National Institutes of Health, USA).

Thermal analysis of the nanofibers

Differential Scanning Calorimetry (DSC822e, Mettler Toledo, Switzerland) was used to investigate thermal characterization of the electrospun fibers. Samples were heated from −50 to 250 °C at a 10 °C/min heating rate under nitrogen flow of 50 mL/min.

[3-(4,5-dimethylthiazol-2-yl)-2,5-d diphenyltetrazolium bromide] (MTT) assays

To measure the cytotoxicity of nanofibers toward mouse fibroblasts, the sterilized photocrosslinked MACS-based nanofibers were incubated in culture medium at an extraction ratio of 6.0 cm[2]/mL for 24 h at 37 °C, after which the nanofibers were removed and the extraction medium was obtained.

200 μL of L929 cell suspension was seeded in 96–well plate at a concentration of 10^5 cells/well. After incubation at 37 °C for 1 day, the culture medium was used instead of the extraction medium. After 1 day, the extract was removed and 10 μL of MTT solution was added to each well. L929 cells were allowed to incubate at 37 °C (5% CO_2) for 4 h, and then the formazan reaction products were dissolved in dimethyl sulfoxide and the plates were shaken for 10 min. The optical density of the formazan solution was read on an ELISA reader at 490 nm.

Dulbecco's modified eagle medium (DMEM) containing 10% fetal bovine serum (FBS) was used as negative control for toxicity.

The resulting values were expressed as cell viability (mean value ± standard deviation). The comparison between the values was made through ANOVA one-way analysis, with $P < 0.05$ considered significant. Analysis was performed using Origin software (7.0 SRO, Northampton, MA, USA).

Cell cultures

HEK 293T cells were cultured in growth medium containing DMEM, 10% fetal bovine serum, 100 U/mL of penicillin, 100 mg/mL of streptomycin and 2 mM/L L-glutamine. HEK 293T cells were incubated at 37 °C in a humidified atmosphere in the presence of 5% CO_2. Photocrosslinked MACS-based mats (a thickness of ~ 0.2 mm) were fixed on cover slips, sterilized and then extensively washed with sterile PBS prior to transfer to 24-well plates. HEK 293T cells suspension with 4.0×10^4 cells/mL were seeded on the mats. The cells were then incubated for 48 h, and investigation of the cells was conducted using a fluorescence microscope. Cells on tissue culture plastic were used as a control group.

Results and discussion

In this research, unsaturated methacrylate groups were introduced onto the chitosan backbones as side groups to prepared nanofiber precursors for the subsequent UV crosslinking process. The synthesis of MACS was achieved by the Michael addition reaction between $–NH_2$ of CS and the acrylate group of EGAMA. ^{1}HNMR of MACS and CS are illustrated in Fig. 1. Methacrylation by the Michael addition is confirmed by ^{1}H NMR, as indicated by the appearance of proton signals of the double bond of the methacrylate group at δ 5.7 ppm and δ 6.1 ppm, as well as methyl groups of methacrylate at δ 1.9 ppm. In addition, N-methacrylation can be identified as a reduction in peak area at δ 3.1 ppm (H-2 of GlcN) in the ^{1}H NMR spectrum. Based on the assignment of the ^{1}H NMR spectrum, the degree of substitution of MACS is calculated as DS $= 0.328 \times I_{1.9}/I_{2.0}$, where $I_{1.9}$ is the integral of the methyl protons at δ 1.9 ppm, and $I_{2.0}$ is the integral of the methyl protons of $–NHCOCH_3$ at δ
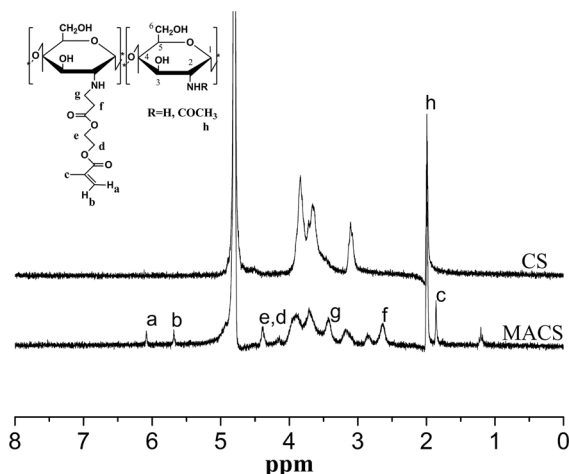

Fig. 1 ^{1}HNMR spectra of MACS in D_2O and CS in CD_3COOD/D_2O

2.0 ppm. The calculated DS is 0.11, which means that 16.4% of the $–NH_2$ group is substituted by methacrylate group. Other peaks were ascribed as follows. 4.38 (e, d, $–COO–CH_2–CH_2OCO–$), 3.7–4.0 (H-3,4,5,6 of GlcN and GlcNAc), 3.4 (g, $N–CH_2–$ of N-alkyl group), 3.2 (H-2 of GlcNAc), 2.9 (g, H-2 of alkylated GlcN), 2.6 (f, $–CH_2COO–$), 2.0 (h, $–NHCOCH_3$).

Electrospinning from pure MACS aqueous solution is highly desirable because it generates pure MACS naonofibers in an environmentally friendly manner. However, only micro- and nanoparticles instead of ultrafine fibers were observed (Fig. 2a), when pure MACS aqueous solution was subjected to electric field force regardless of viscosity or conductivity of the MACS solution. This can be ascribed to two aspects of the difficulty of electrospinning chitosan. First, chitosan chains are closely overlapped and cannot form effective chain entanglements, due to its polycationic nature and semi-rigid chain structure (Desai et al. 2008; Pakravan et al. 2011). Second, chitosan solution displays high electrical conductivities, unacceptably large for electrospinning, which requires jets to experience deep atomization to break into polydisperse eletrosprays (Subramanian et al. 2005). So, an effort was made to enhance the chain entanglements in the chitosan solution and to decrease the conductivity of the chitosan solution. A suitable candidate as a non-ionogenic partner for electrospinning of MACS is PVA, which has the ability to produce nanofibers because of its viscoelastic properties (Rathna et al. 2011). Figure 2 shows SEM images of MACS/PVA
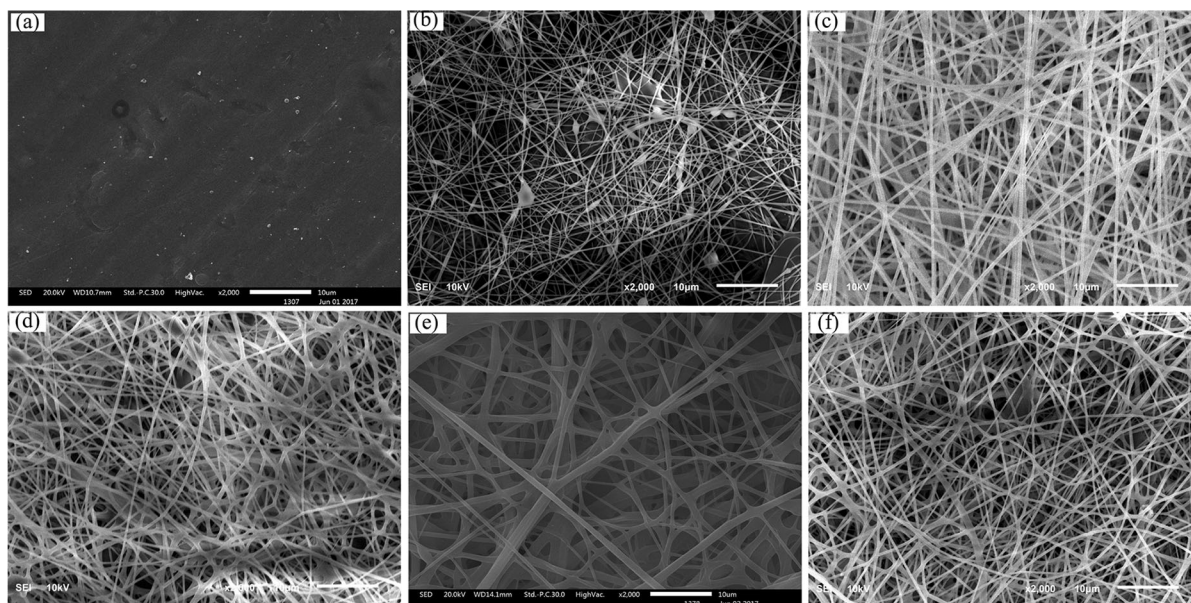
Fig. 2 Effect of the composition of spinning solution on the morphology of MACS/PVA nanofibers. MACS/PVA weight ratio: **a** 100/0; **b** 75/25; **c** 50/50; **d** 25/75; **e** 0/100; **f** 50/50, after UV irradiation

nanofibrous mats with different mass ratios. It is clear that the morphology depends on the content of PVA. As depicted in Fig. 2b, a mixture of thin fibers and beads were observed when the MACS/PVA weight ratio was 75/25. However, when MACS content was less than 50%, the MACS/PVA nanofibers exhibited a more regular morphology and a smooth surface, which made the electrospinning relatively easy.

In many applications, the effect of the average electrospun fiber diameter and its uniformity on the nanofibers' performance is important. Figure 3 presents the diameter distribution of MACS/PVA nanofibers. By statistical calculation, the average diameter of MACS/PVA nanofiber progressively increased from 162 to 476 nm when MACS content gradually fell from 75/25 to 25/75, and fiber diameter distribution became increasingly wider.

It is well documented that the structure and morphology of electrospun fibers are influenced by solution properties such as polymer content, viscosity and conductivity (Bhattarai et al. 2005). The viscosity as a function of the mass ratio of MACS/PVA in the mixed solutions is shown in Fig. 4. As the figure shows, the viscosity of the MACS/PVA solution obviously increased from 0.60 to 1.14 Pa S with the increase of PVA content; the increased viscosity can be ascribed to the increased interactions and

entanglements between polymer chains as a result of increasing concentration of PVA. Correspondingly, as shown in Fig. 2, a transformation from beaded fibers to uniform fibers took place as the PVA increased. When the MACS/PVA weight ratio was high and the viscosity of the blend solution was thus lowered below the limit, the polymer chain entanglements were not enough to form the fiber and beaded fibers were often produced. However when the viscosity of the blend solutions increased due to an increase of PVA content, gradual increase of intra/inter molecular chain entanglement in MACS/PVA solution favored the electrospinnability of the MACS. Similar results have also been reported by others (Li and Hsieh 2006). At the same time, improved of viscosity of the MACS/PVA solution may also contribute to an increase of fiber diameter. The conductivity of MACS/PVA solutions is also presented in Fig. 4. The conductivity of the MACS/PVA blend solutions rose from 1.13 to 2.91 mS/cm as MACS content increased. Because MACS is a polycation, while PVA is a non-ionogenic polymer, increased MACS content could result in an increase of solution conductivity. As mentioned above, high electrical conductivity was unacceptable for electrospinning of the chitosan solution, so when PVA content increased, the conductivity of the MACS/PVA solution was gradually reduced to favor
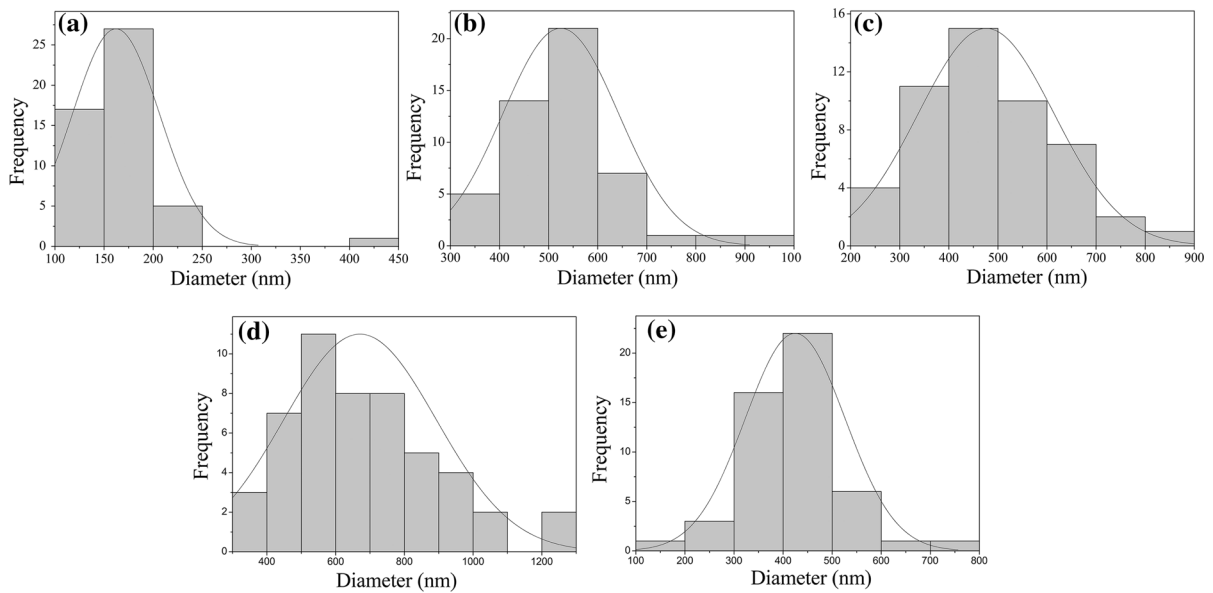
Fig. 3 Diameter distribution of nanofibers for different compositions. MACS/PVA weight ratio: **a** 75/25; **b** 50/50; **c** 25/75; **d** 0/100; **e** 50/50, after UV irradiation
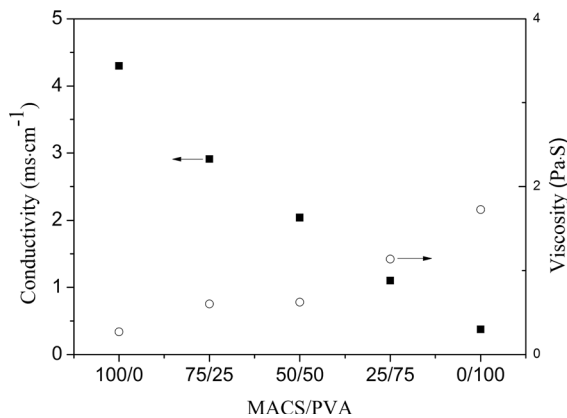

Fig. 4 Conductivity and viscosity of the MACS/PVA blend aqueous solutions

Fig. 5 DSC curves of MACS, PVA, and the nanofibrous membranes with different MACS/PVA weight ratios. *a* 100/0; *b* 50/50; *c* 25/75; *d* 0/100; *e* 50/50 after UV irradiation

the electrospinning of MACS. On the other hand, viscosity of MACS/PVA solution was improved to enhance chain entanglements that occurred between the MACS and PVA. In this way, fine fibers were obtained. The studies based on MACS/PVA blends indicated that it is essential for polymer solutions to have the desired viscosity and conductivity to form smooth nanofibers. The increase in average diameter and broader distribution with decreased MACS content may be due to the increase of viscosity and lower conductivity of the MACS/PVA blend solution. Both
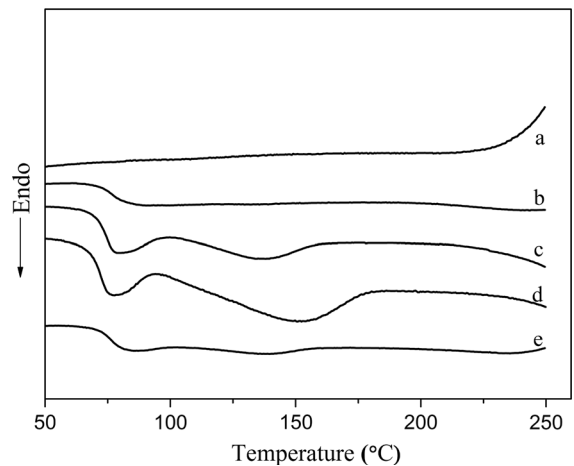
effects resulted in lower stretching rate and subsequently thicker fibers.

The SEM micrographs of fibrous mats after UV irradiation are also illustrated in Fig. 2. As expected, distinct morphological changes were not observed in the electrospun mats after irradiation.

DSC results of MACS, PVA and spun fibers can be found in Fig. 5. In DSC measurements, the second heating run was used. As observed, glass transition
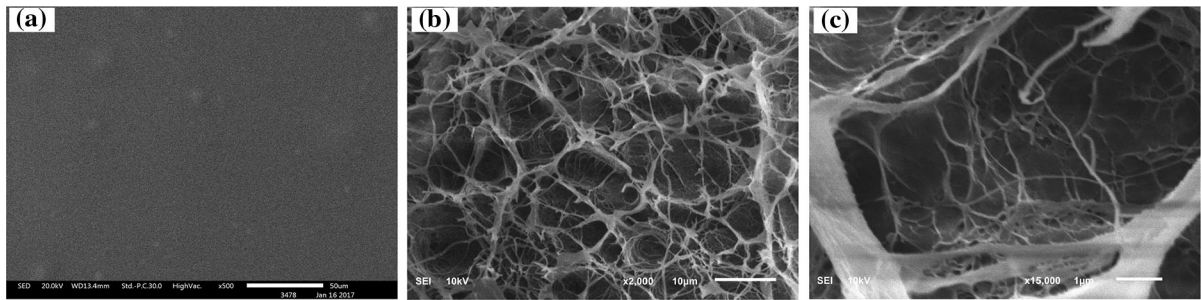
Fig. 6 SEM micrographs of the nanofibers (MACS/PVA = 50/50) with/without UV irradiation after water immersion at 37 °C. **a** Without UV irradiation; **b** with UV irradiation, ×2000 magnification; **c** with UV irradiation, ×15,000 magnification

temperature (T_g) of the MACS was not detected, possibly owing to different characteristics of natural polysaccharides, such as crystallinity, molecular weight and deacetylation degree, from different sources or extraction methods (Neto et al. 2005). MACS/PVA nanofibers displayed Tg around 70 °C and the T_g slightly increased from 71 to 77 °CC as the MACS/PVA weight ratio increased from 0/100 to 50/50. This was possibly due to intermolecular interactions via hydrogen bonds between MACS and PVA limiting movement of the molecular chain segment. In Fig. 5, the PVA presents a melting peak (T_m) at 150 °C. However, for MACS/PVA blends, the endothermic curve broadened and shifted to the lower temperature as MACS content increased. The X-ray diffraction results (see the X-ray diffraction analysis section in the supporting information file) indicated that the introduction of MACS decreased the crystallinity of MACS/PVA blends, which can be attributed to the fact that ordered chain associations of PVA were hindered by the hydrogen bonding interaction between MACS and PVA during electrospinning process (Cay et al. 2014). However, after photopolymerization, MACS/PVA (50/50) nanofibers showed weak Tm peaks around 140 °C, indicating that photocrosslinking could efficiently increase the crystallinity of PVA electrospun nanofibers by increasing hydrogen bonding interactions between the chains and forming a more stable organizing structure.

Pore size and porosity of electrospun fibrous structures play an important role in cell attachment, proliferation and migration for tissue engineering. Although electrospun mats have nanofibrous structures similar to the natural extracellular matrix and can support cell attachment and growth, poor cellular infiltration has been an ongoing problem owing to the
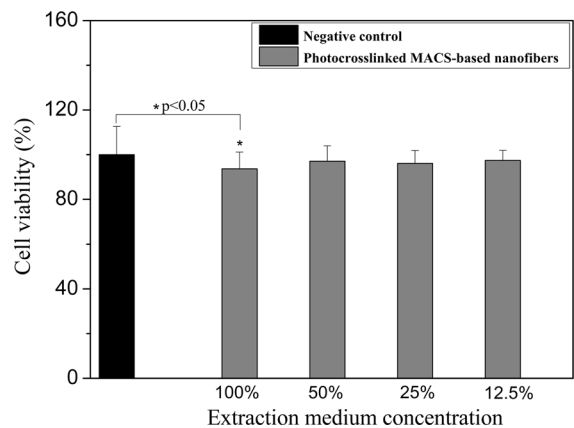

Fig. 7 Plots of cell viability obtained from photocrosslinked MACS-based nanofibers and negative control, respectively

mats having a pore size smaller than typical cellular diameters, limiting cell migration within the nanofibrous scaffold. This can lead to a situation in which the scaffold surface is always covered by a membrane of cells while cells are seldom observed within the scaffold, a circumstance which is not suitable for tissue engineering of three-dimensional tissues (Tuzlakoglu et al. 2011). To obtain micro-pore mats, PVA was chosen as a template polymer to aid electrospinning of MACS to get nanofibers due to its excellent electrospinnability and biocompatibility (Jannesari et al. 2011; Millon et al. 2008). The PVA could be easily removed by immersion in water. Here, photocrosslinked MACS/PVA nanofibers were prepared and then incubated in distilled water at 37 °C for 48 h to remove the PVA.

According to previous work (Liu et al. 2009), the as-spun pure PVA nanofibers were dissolved immediately when immersed in an aqueous environment, owing to the water-solubility of the PVA nanofibers.
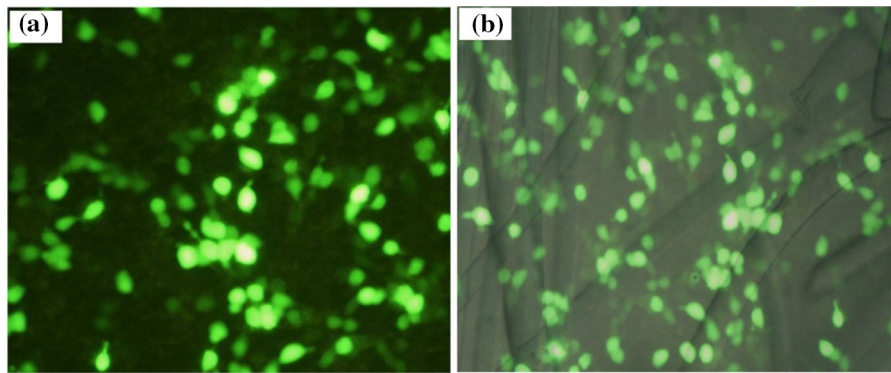
Fig. 8 Fluorescent images of HEK 293T cells cultured under different conditions. **a** Negative control (without nanofibers); **b** photocrosslinked MACS-based mats

Here, the vinyl groups of the MACS molecular chain were crosslinked by UV irradiation to form water-insoluble MACS networks, while PVA without crosslinking could dissolve in water to be removed from fibers. ATR-FTIR results showed that nearly all PVA was removed after the soaking process (shown in the supporting information). Figure 6 presents the SEM images of the nanofibers with and without UV polymerization after water immersion at 37 °C for 48 h. It can be seen that uncrosslinked MACS/PVA nanofiber (50/50) dissolved in water and lost its nanofibrous structure (Fig. 6a). However, photocrosslinked MACS-based mats kept their micropore structure with many fibrils (Fig. 6b-c), and the micrometer-size pores in the electrospun mats were clearly visible.

The photocrosslinked MACS-based mats had a tensile strength of 2.36 ± 0.11 MPa and water-uptake of 6.41 ± 0.65 g/g (shown in the supporting information).

In vitro cytotoxic tests were carried out as an initial verification of the biocompatibility for biomedical materials, with an eye to future applications of biomaterials in tissue engineering. Here, in vitro cytotoxicity of photocrosslinked MACS-based nanofibers was evaluated with L929 cells, as shown in Fig. 7. There was no statistically significant difference ($p < 0.05$) between photopolymerized MACS-based mats and the negative control group when diluted extract concentration at 50% or below 50% was adopted. Although statistical analysis indicated a significant difference ($p < 0.05$) between cytotoxicity of photopolymerized MACS-based mats and the negative control group when 100% extract was used,

cell viability could still be more than 90% of control group. According to International Standard ISO 10993-5 (2009), reduction of cell viability by more than 30% is considered a cytotoxic effect. So, the photopolymerized MACS-based mats were not cytotoxic to L929 cells, which suggests they were biocompatible and suitable for biomedical applications.

Our previous work revealed good adherence and proliferation of the L929 cells on the surface of mats (Zhou et al. 2008). However, cellular infiltration into the nanofibers was constrained due to small pore sizes, which led to a non-uniform cellular distribution among the nanofibers, limiting vascularization and tissue growth (Khorshidi et al. 2016). Figure 8 shows fluorescent images of HEK 293T cells cultured under different conditions. The images show HEK 293T cells at various penetration levels with in-focus cells and out-of-focus cells, indicating various depths throughout the mats (Fig. 8b). The results indicated that the highly micro-porous structure of MACS-based mats allowed for cellular migration into the 3D matrix, which could play a key role in scaffolds for tissue engineering and 3D cell culture (Wingate et al. 2012).

Conclusions

In the present study, photocrosslinkable nanofibrous scaffolds based on MACS were successfully prepared by photocrosslinking electrospun MACS/PVA mats, then subsequently removing PVA from the nanofibers. SEM images showed that MACS/PVA nanofibrous mats had smaller diameters and narrower diameter

distributions as the MACS/PVA weight ratio decreased. DSC results demonstrated the hydrogen bonding interaction between MACS and PVA molecular chains. The photopolymerized MACS-based nanofibrous scaffolds had micro-porous structures with many fibrils after removing PVA with water. The results of in vitro cytotoxicity assessment suggested photocrosslinked MACS-based mats were biocompatible. More interesting, cell culture results indicated that the highly micro-porous structure of MACS-based mats allowed for cellular migration into the 3D matrix. The photocrosslinked MACS-based mats thus have potential applications as skin replacement materials.

References

Alipour SM, Nouri M, Mokhtari J, Bahrami SH (2009) Electrospinning of poly (vinyl alcohol)-water-soluble quaternized chitosan derivative blend. Carbohydr Res 344:2496–2501

Anjum S, Arora A, Alam MS, Gupta B (2016) Development of antimicrobial and scar preventive chitosan hydrogel wound dressings. Int J Pharm 508:92–101

Antunes BP, Moreira AF, Gaspar VM, Correia IJ (2015) Chitosan/arginine–chitosan polymer blends for assembly of nanofibrous membranes for wound regeneration. Carbohydr Polym 130:104–112

Bhattarai N, Edmondson D, Veiseh O, Matsen FA, Zhang M (2005) Electrospun chitosan-based nanofibers and their cellular compatibility. Biomaterials 26:6176–6184

Cay A, Miraftab M, Kumbasar EPA (2014) Characterization and swelling performance of physically stabilized electrospun poly (vinyl alcohol)/chitosan nanofibres. Eur Polym J 61:253–262

Desai K, Kit K, Li J, Zivanovic S (2008) Morphological and surface properties of electrospun chitosan nanofibers. Biomacromol 9:1000–1006

Ding F, Deng H, Du Y, Shi X, Wang Q (2014) Emerging chitin and chitosan nanofibrous materials for biomedical applications. Nanoscale 6:9477–9493

Gao X, Zhou Y, Ma G, Shi S, Yang D, Lu F, Nie J (2010) A water-soluble photocrosslinkable chitosan derivative prepared by Michael-addition reaction as a precursor for injectable hydrogel. Carbohydr Polym 79:507–512

Hirai A, Odani H, Nakajima A (1991) Determination of degree of deacetylation of chitosan by ^{1}H NMR spectroscopy. Polym Bull 26:87–94

Jannesari M, Varshosaz J, Morshed M, Zamani M (2011) Composite poly (vinyl alcohol)/poly (vinyl acetate) electrospun nanofibrous mats as novel wound dressing matrix for controlled release of drugs. Int J Nanomed 6:993–1003

Jayakumar R, Prabaharan M, Sudheesh Kumar PT, Nair SV, Tamura H (2011) Biomaterials based on chitin and chitosan in wound dressing applications. Biotechnol Adv 29:322–337

Khorshidi S, Solouk A, Mirzadeh H, Mazinani S, Lagaron JM, Sharifi S, Ramakrishna S (2016) A review of key challenges of electrospun scaffolds for tissue-engineering applications. J Tissue Eng Regen Med 10:715–738

Kurpinski KT, Stephenson JT, Janairo RRR, Lee H, Li S (2010) The effect of fiber alignment and heparin coating on cell infiltration into nanofibrous PLLA scaffolds. Biomaterials 31:3536–3542

Lee KY, Jeong L, Kang YO, Lee SJ, Park WH (2009) Electrospinning of polysaccharides for regenerative medicine. Adv Drug Deliv Rev 61:1020–1032

Leung V, Hartwell R, Elizei SS, Yang HJ, Ghahary A, Ko F (2014) Postelectrospinning modifications for alginate nanofiber-based wound dressings. J Biomed Mater Res B 102:508–515

Li L, Hsieh YL (2006) Chitosan biocomponent nanofibers and nanoporous fibers. Carbohydr Res 341:374–381

Li HY, Wang MC, Williams GR, Wu JZ, Sun XZ, Lv Y, Zhu LM (2016a) Electrospun gelatin nanofibers loaded with vitamins A and E as antibacterial wound dressing materials. RSC Adv 6:50267–50277

Li J, Wu Y, Zhao L (2016b) Antibacterial activity and mechanism of chitosan with ultra high molecular weight. Carbohydr Polym 148:200–205

Liu Y, Bolger B, Cahill PA, McGuinness GB (2009) Water resistance of photocrosslinked polyvinyl alcohol based fibers. Mater Lett 63:419–421

Millon LE, Guhados G, Wan W (2008) Anisotropic polyvinyl alcohol bacterial cellulose nanocomposite for biomedical applications. J Biomed Mater Res B 86B:444–452

Neto CGT, Giacometti JA, Job AE, Ferreira FC, Fonseca JLC, Pereira MR (2005) Thermal analysis of chitosan based network. Carbohydr Polym 62:97–103

Ohkawa K, Cha D, Kim H, Nishida A, Yamamoto H (2004) Electrospinning of chitosan. Macromol Rapid Commun 25:1600–1605

Pakravan M, Heuzey MC, Ajji A (2011) A fundamental study of chitosan/PEO electrospinning. Polymer 52:4813–4824

Rathna GVN, Jog JP, Gaikwad AB (2011) Development of non-woven nanofibers of egg albumen-poly (vinyl alcohol) blends: influence of solution properties on morphology of nanofibers. Polym J 43:654–661

Rieger KA, Birch NP, Schiffman JD (2013) Designing electrospun nanofiber mats to promote wound healing- a review. J Mater Chem B 1:4531–4541

Song DW, Kim SH, Kim HH, Lee KH, Ki CS, Park YH (2016) Multi-biofunction of antimicrobial peptide-immobilized silk fibroin nanofiber membrane: implications for wound healing. Acta Biomater 39:146–155

Subramanian A, Vu D, Larsen GF, Lin HY (2005) Preparation and evaluation of the electrospun chitosan/PEO fibers for potential applications in cartilage tissue engineering. J Biomater Sci Polym Ed 16:861–873

Sundararaghavan HG, Metter RB, Burdick JA (2010) Electrospun fibrous scaffolds with multiscale and photopatterned porosity. Macromol Biosci 10:265–270

Tang R, Yu Z, Zhang Y, Qi C (2016) Synthesis, characterization, and properties of antibacterial dye based on chitosan. Cellulose 23:1741–1749

Tuzlakoglu K, Santos MI, Neves N, Reis RL (2011) Desigh of nano- and microfiber combined scaffolds by electrospinning of collagen onto starch-based fiber meshes: a man-made equivalent of natural extracellular matrix. Tissue Eng Part A 17:463–473

Uppal R, Ramaswamy GN, Arnold C, Goodband R, Wang Y (2011) Hyaluronic acid nanofiber wound dressing-production, characterization, and in vivo behavior. J Biomed Mater Res B 97B:20–29

Williams CG, Malik AN, Kim TK, Manson PN, Elisseeff JH (2005) Variable cytocompatibility of six cell lines with photoinitiators used for polymerizing hydrogels and cell encapsulation. Biomaterials 26:1211–1218

Wingate K, Bonani W, Tan Y, Bryant SJ, Tan W (2012) Compressive elasticity of three-dimensional nanofiber matrix directs mesenchymal stem cell differentiation to vascular cells with endothelial or smooth muscle cell markers. Acta Biomater 8:1440–1449

Zarandi MA, Zahedi P, Rezaeian I, Salehpour A, Gholami M, Motealleh B (2015) Drug release, cell adhesion and wound healing evaluations of electrospun carboxymethyl chitosan/polyethylene oxide nanofibres containing phenytoin sodium and vitamin C. IET Nanobiotechnol 9:191–200

Zhang KH, Qian YF, Wang HS, Fan LP, Huang C, Mo XM (2011) Electrospun silk fibroin-hydroxybutyl chitosan nanofibrous scaffolds to biomimic extracellular matrix. J Biomater Sci Polym Ed 22:1069–1082

Zhou YS, Yang DZ, Nie J (2006) Electrospinning of chitosan/poly (vinyl alcohol)/acrylic acid aqueous solutions. J Appl Polym Sci 102:5692–5697

Zhou YS, Yang DZ, Chen XM, Xu Q, Lu F, Nie J (2008) Electrospun water-soluble carboxyethyl chitosan/poly (vinyl alcohol) nanofibrous membrane as potential wound dressing for skin regeneration. Biomacromol 9:349–354